

The Linear Combination of Bulk Bands-Method for Electron and Hole Subband Calculations in Strained Silicon Films and Surface Layers

Viktor Sverdlov, Oskar Baumgartner,
Hans Kosina, and Siegfried Selberherr
Institute for Microelectronics, TU Wien
Gußhausstraße 27-29
A-1040 Wien, Austria
Email: sverdlov|baumgartner|kosina|selberherr
@iue.tuwien.ac.at

Franz Schanova
Christian Doppler Laboratory for TCAD
at the Institute for Microelectronics, TU Wien
Gußhausstraße 27-29
A-1040 Wien, Austria
Email: schanova@iue.tuwien.ac.at

David Esseni
DIEGM, Via delle Scienze
I-33100 Udine, Italy
Email: Esseni@uniud.it

Abstract—A generalization of the “Linear Combination of Bulk Bands” method for the calculation of the electron and hole subband structure including strain and spin-orbit interaction is presented. Using the full band structure obtained numerically with the empirical pseudopotential method it is demonstrated that, contrary to the effective mass approximation, the unprimed subbands with the same quantum number in a (001) thin silicon film are not equivalent. It is shown that shear strain modifies the subband effective masses and introduces a large splitting between the unprimed subbands. The generalized method provides accurate subband dispersions for holes demonstrating a large potential for applications.

I. INTRODUCTION

Strain and hybrid orientation techniques are among the most important concepts to increase the performance of modern MOSFETs. The reason for the mobility enhancement lies in the band structure modification caused by stress. Modification of the subband structure of inversion channels is the reason for improved transport characteristics of strained devices. Accurate modeling of the subband structure is mandatory in modern TCAD tools in order to be able to describe MOSFET performance enhancement. The LCBB method in its original version did not include stress and was not able to describe the valence band due to lack of spin-orbit interaction. In this work we generalize the “Linear Combination of Bulk Bands” (LCBB) method [1] to include strain and spin-orbit coupling.

II. CONDUCTION BAND IN SILICON

The subband structure in a confined system must be based on accurate bulk bands of Si including strain. The conduction band in Si is commonly approximated by three pairs of equivalent valleys with their minima located close to the X -points of the Brillouin zone. Close to the minima the electron dispersion is well described by the effective mass approximation with the two transversal masses m_t and the longitudinal mass m_l . At higher electron energies the non-parabolicity parameter (typically $\alpha = 0.5 \text{ eV}^{-1}$) has to be introduced to describe deviations from the density of states of the purely

parabolic dispersion. In ultra-thin body (UTB) FETs, however, the band non-parabolicity affects the subband energies substantially, and it was recently indicated that anisotropic, direction-dependent non-parabolicity could explain a peculiar mobility behavior at high carrier concentrations in a FET with (110) UTB orientation [2]. Therefore, a more refined description of the conduction band minima beyond the usual single-band non-parabolic approximation is needed. Another reason to challenge this standard approximation is its inability to address properly the band structure modification under stress. Indeed, shear strain also modifies substantially both the longitudinal [3], [4] and transversal [3]–[6] effective masses. Any dependence of the effective masses on stress is neglected within the single-band description of the conduction band and can only be introduced phenomenologically. In order to describe the dependence of the effective mass on stress a single-band description is not sufficient, and coupling to other bands has to be taken into account.

Several options are available. The $\mathbf{k}\cdot\mathbf{p}$ theory is a well established method to describe the band structure analytically [7]. Recently, a 30 bands $\mathbf{k}\cdot\mathbf{p}$ theory was introduced [8]. Although universal, it cannot provide an explicit analytical solution for the energy dispersion. An efficient two-band $\mathbf{k}\cdot\mathbf{p}$ theory [3], [4], [6], [9] reproduces the band structure at low energies quite well as shown in Fig. 1 where the conduction band dispersion of the [001] valleys computed with several methods in [100] and [110] directions are compared.

We use the empirical nonlocal pseudopotential method (EPM) for numerical band structure calculations. The parameters of the EPM are adjusted in order to reproduce the measurable quantities of semiconductors, energy gap and effective masses, as well as results of the first principle density functional calculations. The method includes spin-orbit coupling. In our calculations of the silicon band structure we used the parameters from [12]. As follows from Fig. 1, the EPM results are the most accurate, when compared to the first principle density functional (DFT) band structure calculations

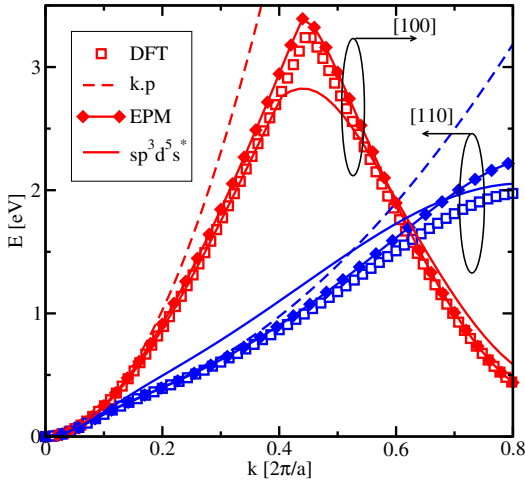


Fig. 1. Comparison of bulk dispersion relations close at the minimum of the [001] valleys of the conduction band in [100] and [110] directions. DFT [10] and EPM [3] results are similar, while the $sp^3d^5s^*$ tight-binding model [11] slightly underestimates anisotropy.

obtained with the VASP [10].

An alternative method for band structure calculations based on empirical tight-binding models has recently gained popularity. Already the sp^3s^* tight-binding model allows to reproduce reasonably well the valence band structure of silicon [13]. Recent development and calibration of a more sophisticated $sp^3d^5s^*$ model [11] has improved the reproducibility of the silicon conduction band. Agreement between the band structures obtained from the EPM and the $sp^3d^5s^*$ model with the parameters from [11] is reasonably good as shown in Fig. 1. However, the $sp^3d^5s^*$ tight-binding model slightly underestimates the anisotropy of the conduction band. The effect is clearly visible in Fig. 2, which demonstrates that the EPM gives a more pronounced conduction band warping than the $sp^3d^5s^*$ tight-binding model. In addition, an accurate

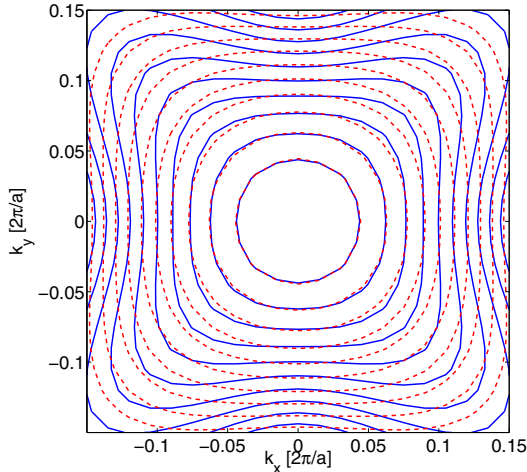


Fig. 2. Comparison between the k_x, k_y bulk dispersion relations at the minimum k_0 . The contour lines are spaced every 50 meV. Solid lines correspond to the EPM and the dashed lines to the $sp^3d^5s^*$ model.

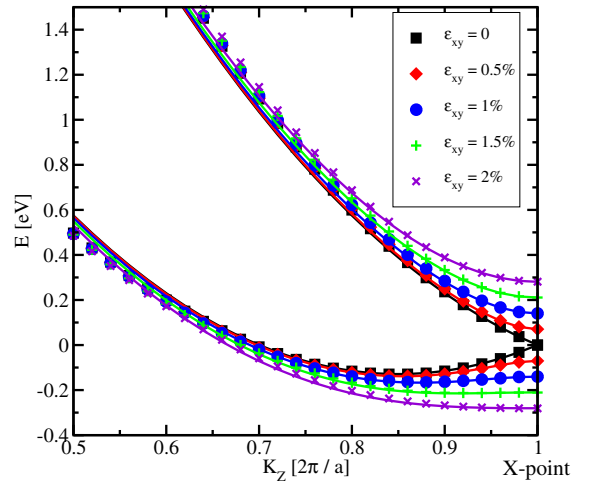


Fig. 3. The k_z dispersions obtained from the empirical pseudopotential calculations for several values of shear strain. Shear strain in [110] direction opens the gap between the two lowest conduction bands of the [001] valleys at the X -point. It prompts the minimum position to move closer to the X -point.

calibration of the parameters of the $sp^3d^5s^*$ model to describe the modification of the conduction band in strained Si is still missing, while the EPM calculations can be readily generalized to include strain [12]. Fig. 3 shows the dispersion of the [001] valley in z direction as a function of shear strain ε_{xy} obtained with the EPM solver [14].

III. “LINEAR COMBINATION OF BULK BANDS” METHOD

In the LCBB method the solution

$$\psi(\mathbf{r}) = \sum_{n,k_z} A_n(\mathbf{k}, k_z) |n, \mathbf{k}, k_z\rangle \quad (1)$$

of the Schrödinger equation $(H_0 + V(z)) \psi_E(\mathbf{r}) = E \psi_E(\mathbf{r})$ with the confinement potential $V(z)$ is obtained using the

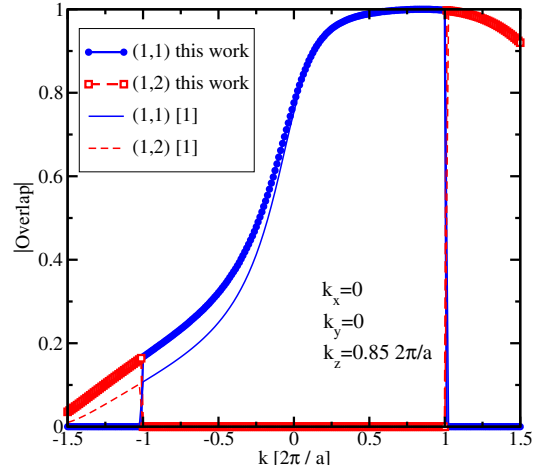


Fig. 4. Comparison of the overlap integrals obtained with the two sets of pseudopotentials from [1] and [3]. (i, j) means the overlap integral between the Bloch functions the conduction bands i and j .

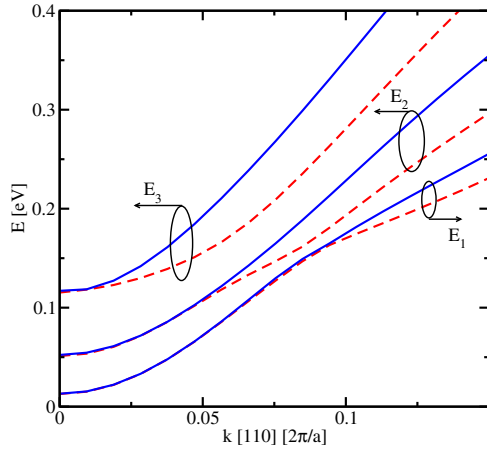


Fig. 5. Dispersion relations of the unprimed subbands for the unstrained (001) 5.4nm thick Si film. The subband degeneracy is lifted for finite momentum in [110] direction.

complete set of the Bloch functions $|n, \mathbf{k}, k_z\rangle$ of the Hamiltonian $H_0 = \frac{\mathbf{p}^2}{2m_0} + U(\mathbf{r})$ of bulk silicon [1]. Therefore, the method is suitable to get the dispersion relations for any confining potential in silicon. In this work we model the thin silicon film of the thickness t by approximating $V(z)$ with a square well potential although the generalization to an arbitrary potential profile is straightforward. The hight of the potential barrier corresponds to the potential energy barrier at the semiconductor-oxide interface.

The advantage of the LCBB method is that it allows to use accurate band structure and Bloch functions obtained by a suitable numerical method without any additional approximation. The Schrödinger equation written in the basis of (1) takes the form [1]:

$$\begin{aligned} \sum_{n,k_z} & \langle n, \mathbf{k}, k_z | V(z) | n, \mathbf{k}, k_z \rangle A_n(\mathbf{k}, k_z) \\ & = (E(\mathbf{k}) - E_{FB}(\mathbf{k}, k_z)) A_n(\mathbf{k}, k_z). \end{aligned} \quad (2)$$

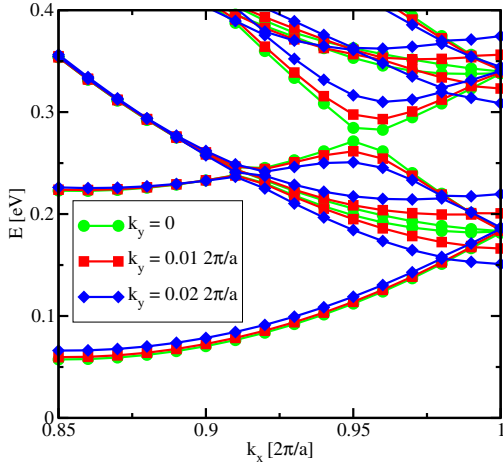


Fig. 6. Primed subband dispersion relations for a (001) unstressed 5.4nm thick Si film in [001] direction. The third valley [1] splits for finite k_y . It indicates that the third valley may originate from the two [100] primed subbands.

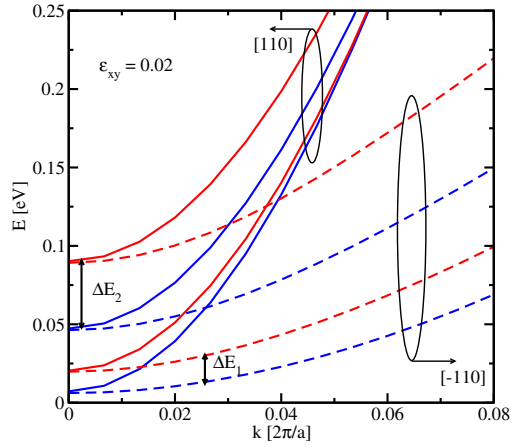


Fig. 7. Strain-induced splitting between unprimed subbands is observed in a (001) 5.4nm thick Si film. Strain dependence of the effective masses results in the difference between the subband dispersions in [110] and [-110] directions.

It is important to stress that in the summation of Eq.(2) k_z must vary in a periodicity interval of the reciprocal lattice vector space along the k_z direction [1]. The matrix element of the confining potential can be expressed via the overlap integrals of the periodic parts of the Bloch functions $\langle u_{n,\mathbf{k},k_z} | u_{n',\mathbf{k},k'_z} \rangle$ as

$$\begin{aligned} & \langle n, \mathbf{k}, k_z | V(z) | n', \mathbf{k}, k'_z \rangle \\ & = \sum_{(\mathbf{g}, g_z)} \langle u_{n,\mathbf{k}-\mathbf{g},k_z-g_z} | u_{n',\mathbf{k},k'_z} \rangle \\ & \quad \times V(k'_z - k_z + g_z) \delta_{\mathbf{k}, \mathbf{k}' + \mathbf{g}}, \end{aligned} \quad (3)$$

where (\mathbf{g}, g_z) is the reciprocal lattice vector and

$$V(k_z) = \int \frac{dz}{L_z} V(z) \exp(ik_z z)$$

is the Fourier harmonic of the confining potential and $\delta_{\mathbf{k}, \mathbf{k}' + \mathbf{g}}$ is the Kronecker's delta [1].

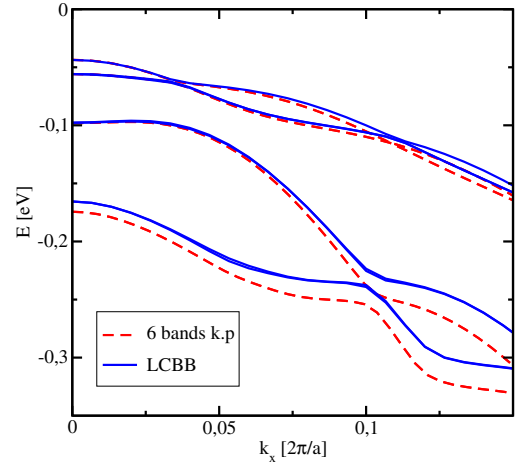


Fig. 8. Dispersion relation of hole subbands in a (001) unstrained Si film of 5.4nm thickness obtained with the LCBB and the 6-bands $\mathbf{k}\cdot\mathbf{p}$ method. Good agreement is achieved thanks to the inclusion of spin-orbit interaction into the EPM full band calculations.

Important ingredients of the LCBB method are the overlap integrals (3) of the periodic parts of the Bloch functions. Overlap integrals of the Bloch functions from the first and second conduction band computed with pseudopotentials from [3] are in excellent agreement with previously published results [1] as demonstrated in Fig. 4. The advantage of the pseudopotential method [3] is that it provides the band structure in strained silicon. The method also includes the spin-orbit coupling which is important to describe the valence band.

IV. RESULTS

We start calculations by investigating the subband structure of a (001) silicon film. The dispersion relations for the unprimed subbands in a 5.4nm thick unstrained Si film in [110] direction are shown in Fig. 5. The subband calculations based on the full-band consideration demonstrate that the two unprimed subbands with the same quantum number, which are completely equivalent in the effective mass approximation, develop quite a difference in energies for finite momentum in [110] direction. This result suggests that even the effective masses of the two unprimed subbands with the same quantum number may be different, an observation that has never been mentioned before.

Dispersion relations of primed subbands in a 5.4nm (001) silicon film are shown in Fig. 6 at $k_y = 0$ and also for nonzero values of k_y . For $k_y = 0$ we can clearly see the third valley with the minimum at the X -point [1], [15]. However, for $k_y \neq 0$ it clearly splits in two branches, with the energy of the lower branch decreasing while increasing k_y and moving away from the X -point in [100] direction. For $k_y = 0.15(2\pi/a)$ and $k_x = 2\pi/a$ the energy of the lower branch becomes equal to the energy of the unprimed subband at the minimum $k_x = 0.85(2\pi/a)$, $k_y = 0$. Similar behavior is observed when the value of k_y is inverted to $k_y \rightarrow -k_y$. This behavior indicates that the third valley originates from a pair of primed subbands with minima along [100] direction.

Next we consider an example of a (001) film stressed along [110] direction. Stress in [110] direction generates the shear strain component which causes a profound modification of the bulk dispersion [3], [4], [6]. Due to the shear strain component the degeneracy between the unprimed subbands with the same quantum number is lifted even at $k_x = k_y = 0$ resulting in a large strain-induced valley splitting (Fig. 7). Substantial differences in the dispersion along [110] (solid lines) and [1-10] (dashed lines) directions indicate strong modification of the effective masses due to strain and reduced thickness [4].

Finally, we have carried the subband calculations for the valence band. The nonlocal pseudopotentials [3], [12] include spin-orbit interaction and thus the generalized LCBB method accurately describes the hole subbands. A comparison of subbands obtained with the LCBB method and the 6-bands $\mathbf{k}\cdot\mathbf{p}$ method is shown in Fig. 8.

V. CONCLUSION

We have generalized the “Linear Combination of Bulk Bands” method for the calculation of the electron and hole

subband structure to include strain and spin-orbit interaction. An accurate band structure obtained numerically with the pseudopotential method is used. It is demonstrated that contrary to the effective mass approximation the unprimed subbands with the same quantum number in a (001) thin silicon film are not equivalent. Shear strain further modifies the effective masses and introduces a large splitting between the unprimed subbands. It is shown that, thanks to the inclusion of the spin-orbit interaction, the LCBB method provides accurate subband dispersions for holes demonstrating the potential of the method for nanoelectronic applications.

ACKNOWLEDGMENT

This work has been supported by the Austrian Science Fund FWF, projects P19997-N14, I79-N16, and SFB IR-ON F2509.

REFERENCES

- [1] D. Esseni and P. Palestri, “Linear combination of bulk bands method for investigating the low-dimensional electron gas in nanostructured devices,” *Phys. Rev. B*, vol. 72, no. 16, p. 165342, Oct 2005.
- [2] K. Uchida, A. Kinoshita, and M. Saitoh, “Carrier transport in (110) nMOSFETs: Subband structure, non-parabolicity, mobility characteristics, and uniaxial stress engineering,” in *IEDM Techn. Dig.*, 2006, pp. 1019–1021.
- [3] E. Ungersboeck, S. Dhar, G. Karlowatz, V. Sverdlov, H. Kosina, and S. Selberherr, “The effect of general strain on band structure and electron mobility of silicon,” *IEEE Trans. Electron Devices*, vol. 54, no. 9, pp. 2183–2190, 2007.
- [4] V. Sverdlov, G. Karlowatz, S. Dhar, H. Kosina, and S. Selberherr, “Two-band $\mathbf{k}\cdot\mathbf{p}$ model for the conduction band in silicon: Impact of strain and confinement on band structure and mobility,” *Solid-State Electron.*, vol. 52, pp. 1563–1568, 2008.
- [5] K. Uchida, T. Krishnamohan, K. C. Saraswat, and Y. Nishi, “Physical mechanisms of electron mobility enhancement in uniaxial stressed MOSFETs and impact of uniaxial stress engineering in ballistic regime,” in *IEDM Techn. Dig.*, 2005, pp. 129–132.
- [6] J. C. Hensel, H. Hasegawa, and M. Nakayama, “Cyclotron resonance in uniaxially stressed silicon. II. Nature of the covalent bond,” *Phys. Rev.*, vol. 138, no. 1A, pp. A225–A238, Apr 1965.
- [7] J. M. Luttinger and W. Kohn, “Motion of electrons and holes in perturbed periodic fields,” *Physical Review*, vol. 97, no. 4, pp. 869–883, 1953.
- [8] D. Rideau, M. Feraille, L. Ciampolini, M. Minondo, C. Tavernier, H. Jaouen, and A. Ghetti, “Strained Si, Ge, and $\text{Si}_{1-x}\text{Ge}_x$ alloys modeled with a first-principles-optimized full-zone $\mathbf{k}\cdot\mathbf{p}$ method,” *Phys. Rev. B*, vol. 74, no. 19, p. 195208, Nov 2006.
- [9] G. L. Bir and G. E. Pikus, *Symmetry and Strain-Induced Effects in Semiconductors*. New York - Toronto: John Wiley & Sons, 1974.
- [10] VASP, *Vienna Ab-initio Simulation Program*, G.Kresse and J. Hafner, *Phys. Rev. B* 47, 558 (1993); *ibid. B* 49, 14251 (1994); G.Kresse and J. Fertmueller, *Phys. Rev. B* 54, 11169 (1996); *Computs. Mat.Sci.* 6, 15 (1996).
- [11] T. B. Boykin, G. Klimeck, and F. Oyafuso, “Valence band effective-mass expressions in the $sp^3d^5s^*$ empirical tight-binding model applied to a si and ge parametrization,” *Physical Review B (Condensed Matter and Materials Physics)*, vol. 69, no. 11, p. 115201, 2004. [Online]. Available: <http://link.aps.org/abstract/PRB/v69/e115201>
- [12] M. M. Rieger and P. Vogl, “Electronic-band parameters in strained $\text{Si}_{1-x}\text{Ge}_x$ alloys on $\text{Si}_{1-y}\text{Ge}_y$ substrates,” *Physical Review B*, vol. 48, no. 19, pp. 14 276–14 287, Nov 1993.
- [13] S. Datta, *Quantum Transport: Atom to Transistor*. Cambridge University Press, 2005.
- [14] V. Sverdlov, E. Ungersboeck, H. Kosina, and S. Selberherr, “Current transport models for nanoscale semiconductor devices,” *Materials Science and Engineering R*, vol. 58, no. 6-7, pp. 228–270, 2008.
- [15] D. Esseni and P. Palestri, “Fullbandbulk quantization analysis reveals a third valley in (001) silicon inversion layers,” *IEEE Electron Device Lett.*, vol. 24, no. 5, pp. 353–355, 2005.